ACS NANO

Defining nanoscience and nanotechnology

ACS Publications
Most Trusted. Most Cited. Most Read.

www.acs.org

ACS NANO

www.acsnano.org

ARTICLE

Discovering the Secret of Diseases by Incorporated Tear Exosomes Analysis *via* Rapid-Isolation System: iTEARS

Liang Hu,[○] Ting Zhang,[○] Huixiang Ma,[○] Youjin Pan, Siyao Wang, Xiaoling Liu, Xiaodan Dai, Yuyang Zheng, Luke P. Lee,* and Fei Liu*

Cite This: https://doi.org/10.1021/acsnano.2c02531

ABSTRACT: Nanoscale small extracellular vesicles (sEVs, exosomes) in tears allow us to investigate the multisignatures of diseases. However, the translations of tear sEVs for biomarker discovery and clinical diagnostics are practically limited by low recovery, long processing time, and small sample volume. Here, we report an incorporated tear-exosomes analysis *via* rapid-isolation system (iTEARS) *via* nanotechnology to discover the secrets of ocular disorders and systemic diseases. We isolate exosomes rapidly with high yield and purity from a few teardrops (~10 μL) within 5 min *via* nanoporous membrane-based resonators for the quantitative detection and biomarker discovery through proteomic and transcriptomic analysis. We have identified 904 proteins, among which 228 proteins are discovered, 426 proteins are detected from exosomes of dry eye disease, and demonstrate CALML5, KRT6A, and S100P for the classification of dry eye disease. We have also investigated 484 miRNAs in tear exosomes and show miR-145-5p, miR-214-3p, miR-218-5p, and miR-9-5p are dysregulated during diabetic retinopathy development. We believe iTEARS can be used for improving molecular diagnostics *via* tears to identify ocular disorders, systemic diseases, and numerous other neurodegenerative diseases and cancer.

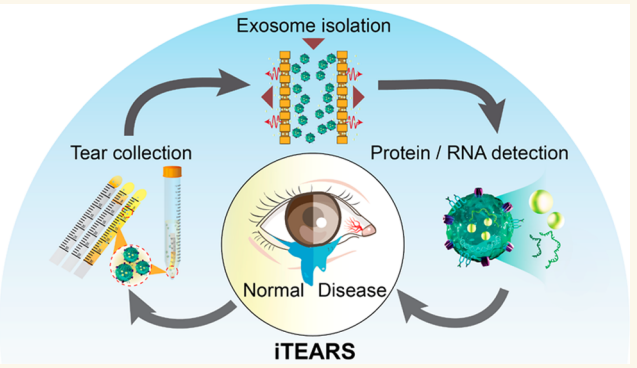

KEYWORDS: *diagnostics, identification, tears, extracellular vesicles, eye diseases, biomarkers, nanotechnology*

Current clinical studies pose significant challenges in distinguishing disease subtypes with accurate molecular signatures and tracking the disease progression in a non-invasive way.[1,2] Since small extracellular vesicles (sEVs, exosomes) reveal specific functions in various biological processes, including immune regulation, angiogenesis, tumor invasion, and cell migration, exosome-based liquid biopsy technology has offered an attractive alternative to disease classification and prognostic prediction.[3,4] As one of the crucial fluid resources for exosome study, tears are secreted from the lachrymal gland for maintaining normal eye physiological activities. Typically, tear film has a volume of about 5−10 μL and shares parts of blood components *via* vascular permeating, indicating a prominent role of tears in deepening our understanding of ocular disorders and systemic diseases.[5,6] In contrast to other ocular fluids, tears are highly accessible for biomarker analysis using the Schirmer test strip,[7] allowing us to discover the molecular signatures of disease and establish the non-invasive diagnostic methods.

To see the world of disease in a drop of tear, significant efforts have been made to detect tear components such as lactoferrin, lysozyme, glucose, and alcohol, for characterizing the pathology states including dry eye symptoms,[8] infections,[9] diabetes,[10] and even drinking.[11] In terms of exosomes, both the morphology and miRNA expression levels of tear exosomes have been reported to provide the basis for the diagnostic application of primary open-angle glaucoma.[12] By identifying the proteins *via* liquid chromatography−mass spectrometry (LC-MS), tear exosomes were found to carry more immune response-related proteins such as copine 1, calmodulin, and erythrocyte band 7 integral membrane protein, Annexin A4,

Received: March 13, 2022
Accepted: May 17, 2022

https://doi.org/10.1021/acsnano.2c02531
ACS Nano XXXX, XXX, XXX−XXX

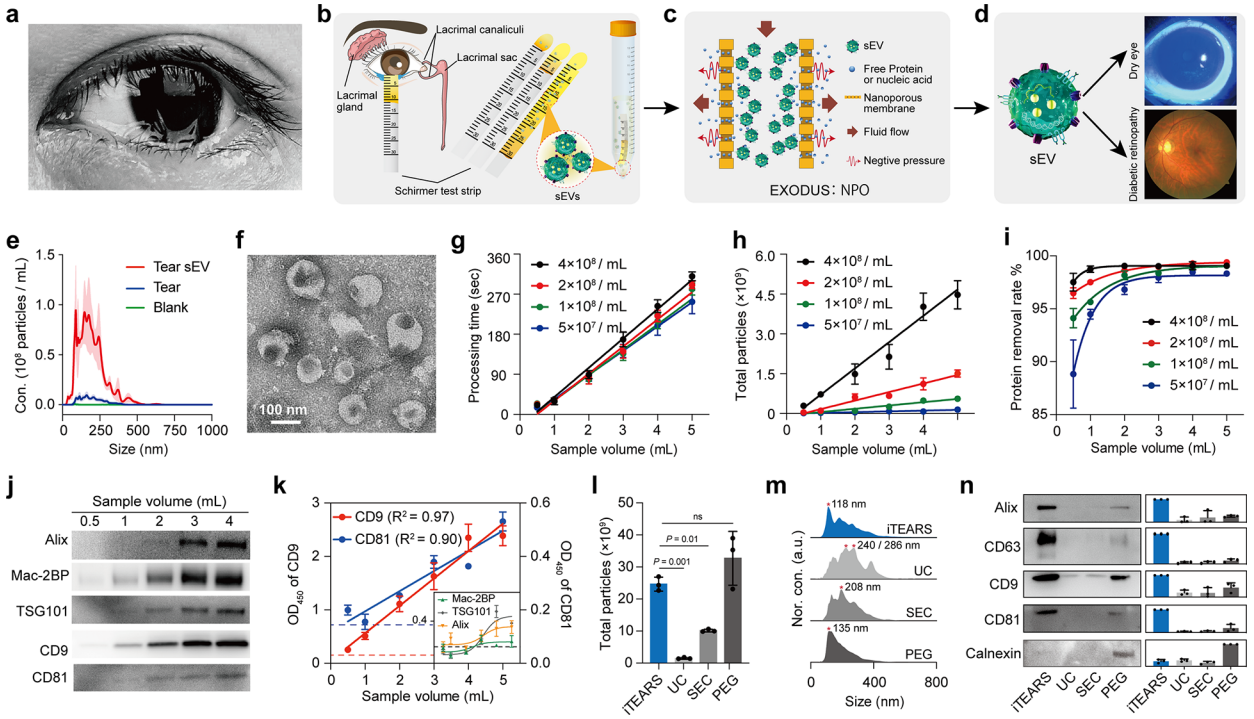

Figure 1. iTEARS for disease detection based on a teardrop. (a, b) Tears collection using the Schirmer test strip, (c) then processed using the EXODUS device on the basis of negative pressure oscillation on nanoporous membranes, and (d) finally used for tear-exosome-based disease detection. (e) Nanoparticle tracking analysis (NTA) measurements of the particle concentration and size distribution of tear suspensions (5 mL), exosome isolates (150 μL), and blank isolates (150 μL, Schirmer paper without tear). Data are shown as mean ± standard error of the mean (SEM), n = 6. (f) Morphology analysis of tear exosomes captured by transmission electron microscopy (TEM). (g) Exosome isolation time, (h) particle amounts, and (i) protein removal rate upon incremental volumes and serially diluted concentrations of the tear suspensions (n = 3, mean ± SEM). (j) Expression pattern of proteins in tear exosomes isolated by iTEARS. Exosomes were obtained from tear suspensions and were loaded with an equal volume of 20 μL. The specific exosomal markers, including Alix, TSG101, CD9, and CD81, and the exosome enriched protein Mac-2BP were selected. (k) Correlation of initial sample volume and on-device immunodetection signals by measuring the OD_{450} values (n = 3, mean ± SEM). Insert represents the OD_{450} of Mac-2BP, TSG101, and Alix. Dashed line represents the limit of detection. (l) Particle yield among different isolation methods (n = 3). Data are shown as mean ± standard deviation (SD). The CV values of 8.9, 17.0, 4.1, and 25.7% for iTEARS, UC, SEC, and PEG precipitation, respectively. (m) Particle size distributions of sEVs were prepared by different methods. The normalized concentration (Nor. con.) profiles are measured by NTA and constructed by the average curve (n = 3). Asterisks indicate the model size peaks. (n) Equal-protein-mass (3 μg) western blot analysis of the exosomal markers (Alix, CD63, CD9, and CD81) and negative marker (Calnexin) in samples prepared by iTEARS and other methods. The right panel shows quantification results of the normalized band intensities from three repeats (mean ± SD). All independent experiments were performed using a tear pool of 4−6 donors.

and Annexin A11 in primary Sjögren's syndrome (pSS) patients.[13,14] Our previous work also shows the diagnostic potential of tear components in dry eye detection by fingerprinting their molecular signals.[15] Moreover, intact exosomes from tears have been demonstrated to convey similar proteins from the cerebrospinal fluid of Multiple Sclerosis patients.[16] They have also been applied in testing breast cancer and monitoring mastectomy treatments by profiling their surface protein biomarkers or embedded miRNA,[17,18] further suggesting the non-invasive diagnostic potential of tear exosomes.

Despite these attractive findings, limited progress has been reported in intensely appreciating the clinical value of tear exosomes due to the practical limitations in sample handling and analytical performance of tear exosomes. Isolation relying on the particle density and size is the most commonly used strategy for purifying exosomes.[19−21] Among these, ultracentrifugation (UC) and size exclusion chromatography (SEC) are the most common methods for isolating tear exosomes.[12,13,22,23] Yet, the low recovery, long processing time, large sample consumption of UC, and the lack of enrichment capacity of SEC hinder the development of biomarker discovery and sensitive detection. The polymer precipitation method[24] can isolate particles with a high yield but low purity. Flow cytometry[25] can purify EVs on the basis of their chemical properties, but it requires prelabeling the EV populations and additional specialized equipment. Microstructure-based devices have emerged to meet the above challenges in exosome extraction and composition sensing.[26,27] Recently, we have established a series of nanofilter-based platforms for isolating and analyzing exosomes from samples with small volumes such as urine and plasma, showing the efficient performance of these analytical platforms in recognizing various diseases.[28−30] However, because the volumes of tear collected from individuals, especially the patients, are usually minimal, and the contents are relatively complex, techniques for purifying tear exosomes are still urgently needed to decipher the diseases from a teardrop and thus facilitate its diagnostic applications.[18]

Here, we describe an incorporated tear-exosome analysis *via* a rapid-isolation system (iTEARS) to uncover the secrets of diseases from exosomes in a few drops of tear. Using our ultrafast-isolation system based on the negative-pressure-

https://doi.org/10.1021/acsnano.2c02531
ACS Nano XXXX, XXX, XXX−XXX

oscillation strategy and on-device immunodetection, we demonstrate that exosomes could be enriched rapidly (less than 5 min) and quantitively characterized after tear collection using the Schirmer test strip. On-device detection also enables us to obtain the quantitative exosomal signals by targeting antibodies to their membrane proteins. As a clinical application of iTEARS, we have further performed the systematic analysis of exosomes derived from healthy control (HC), dry eye symptom (DES), and dry eye disease (DED) subtypes, including the evaporative dry eye (EDE) and aqueous tear deficient dry eye (ADDE). Results show that differential exosome levels and protein profiling might distinguish HC, EDE, ADDE, and DES. Finally, we have used the iTEARS to discriminate diabetic retinopathy and diabetic mellitus from HC and suggest the potential of tear exosomes and exosomal miRNAs in monitoring disease development. Our iTEARS will be a powerful platform for discovering biomarkers of various diseases *via* exosomes from tears and understanding the clinical pathogenesis to establish tear-exosome-based precision medicine. We also believe iTEARS can be used for improving molecular diagnostics using tears to investigate ocular disorders, systemic diseases, and numerous other neurodegenerative diseases and cancer.

RESULTS AND DISCUSSION

Purification of Tear Exosomes by iTEARS. Tears were collected from healthy individuals using household Schirmer test strips to sample non-invasively. After transferring strips into 5 mL of 1X phosphate-buffered saline (1X PBS) and pre-removal of cell or cell debris, the final tear suspension was processed by iTEARS for exosome purification (Figure 1a,b and Supporting Information Figure S1). We utilized our nanoporous membrane oscillators,[31] which comprise a sample reservoir coupling with a dual nanoporous anodic aluminum oxide (AAO) filter and two outlets connected to the negative-pressure-oscillation (NPO) system (Figure 1c). To achieve fast exosome isolation, the periodic NP switching is applied on two sides of the device, which can drive the sample, entrap exosomes, remove the small fragments (*e.g.*, proteins and nucleic acids), and reduce the bioaggregates on membranes, thus shortening the processing time and extending the range of processing volume. Purified exosomes are then extracted for downstream analysis (Figure 1d).

We first analyzed the size distribution and ultrastructure of tear exosomes to characterize their biophysical features. Nanoparticle tracking analysis (NTA) showed a size distribution mainly ranging from 50 to 300 nm, observing a particle enrichment effect during exosome isolation and negligible background signals induced from test strips (Figure 1e). Transmission electron microscopy (TEM) results also depicted that most purified tear vesicles are intact with classic spherical and cup-shaped structures (Figure 1f), consistent with those reported in previous exosomal studies.[12] The size deviation between the NTA and TEM results could be explicated by fluorescence interference from the Schirmer strips, which could be calibrated by TEM measuring the vesicle size (ranging from 30 to 140 nm with a mean of 77 nm, Figure S2).

We then evaluated the stability and reproducibility of iTEARS by measuring the processing time and the particle yield. Isolation of tear suspension at 2-fold serially diluted concentrations in incremental volumes from 0.5 to 5 mL was performed. As shown in Figure 1g, individual tear samples with crescent volumes raised the time consumption linearly. However, only a slight decrease can be observed on filtration when we diluted the input sample, demonstrating the high inclusiveness of iTEARS in processing samples with various complexities. Similarly, the amounts of particles showed an excellent linear relationship to the input sample volume at all concentrations (Figure 1h), further proving that our method is stable and reproductive during sample handling. Moreover, the entire isolation process could be accomplished within 5 min (Figure 1g), and a constant high protein removal rate (determined by comparing the total protein amount of the samples before and after iTEARS isolation) of approximately 98% was observed when we performed samples without dilution (Figure 1i). Western blot (WB) also showed stronger signals of the total proteins and exosomal markers in samples with higher initial volume (Figure 1j and Figure S3a,b), suggesting a low processing volume of 1 mL for WB analysis. Additionally, we compared the WB signals of exosomal markers and albumin between EVs and tears, resulting in an efficient enrichment and purification effect during tear processing (Figure S3c).

Since the iTEARS enables antibody targeting exosomes while filtering out the small-size free antibodies, we finally showed its performance in quantitative exosomal detection *in situ*. The principle was similar to an enzyme-linked immunosorbent assay (ELISA),[32] and the average operation time is less than 3 h. Comparing the optical density value at 450 nm (OD_{450}) of different compositions, a noise level of 0.05, an incubation time of 30 min, and a minimum washing buffer volume of 3 mL were optimized (Figure S4). To assess the on-device detection linearity, tests using tear-dissolved PBS were conducted. As summarized in Figure 1k, a strong linear correlation between the sample volume and OD_{450} was observed when targeting the membrane proteins such as CD9 (R^2 = 0.97) and CD81 (R^2 = 0.90), yielding a limit of detection (LOD) at 0.5−1 mL of input sample volume (calculated by 3-fold signal-to-noise ratio). We also observed a nonlinear curve for detecting TSG101 and Alix (the endosomal sorting complexes required for transport that play key roles in exosomal biogenesis), suggesting a LOD of 3 mL of input. Besides, the weak signals upon Mac-2BP further suggested that the OD_{450} is suitable for detecting exosomal membrane proteins.

Notably, we can obtain more than 10^9 tear particles (~10^{10} particles/mL) from an individual donor with the iTEARS device, which is 10- to 100-fold higher than SEC and UC (according to the summarized data[33]). To eliminate the experimental bias among other studies, we performed a comparative analysis with the commercial methods for tear EV isolations, including UC, SEC, and PEG precipitation. As shown in Figure 1l, particle amounts with iTEARS were significantly higher than those *via* UC (18.4-fold) and SEC (2.3-fold), while they were comparable with PEG results. Besides, samples with iTEARS and PEG showed a relatively high proportion of small particles (<200 nm), despite the similar particle size range among all methods (Figure 1m). The coefficient of variation of the NTA and Qubit Protein Assay Kit (Figure S3d) measurements further showed technical reproducibility of iTEARS (8.9%, 3.7%). To compare the sEV purity among different isolation methods, we thus performed Western blots with equal-mass proteins to determine the presence of exosome-positive proteins (CD9, CD63, CD81, and Alix) and negative maker (Calnexin) according to the

https://doi.org/10.1021/acsnano.2c02531
ACS Nano XXXX, XXX, XXX−XXX

Table 1. Clinical Data of Dry Eye Patients for the Particle Concentration Study and the Proteomic Study[a]

Group	*n*	Gender (M/F)	Age (years)	OSDI	TBUT	Schirmer I test	Fluorescein staining
				Particle concentration study			
HC	13	4/9	25.30 ± 4.59	5.48 ± 4.75	13.31 ± 1.70	24.27 ± 8.81	0.00 ± 0.00
DES	10	4/6	36.30 ± 13.95	28.63 ± 22.66	9.00 ± 0.94	20.95 ± 6.28	0.30 ± 0.48
EDE	20	6/14	43.7 ± 16.36	33.33 ± 23.89	4.38 ± 1.92	12.58 ± 6.86	1.95 ± 2.56
ADDE	20	5/15	50.7 ± 12.61	31.99 ± 17.61	3.38 ± 1.40	2.04 ± 1.90	3.45 ± 2.70
				Proteomic study			
HC	6	2/4	26.33 ± 1.03	5.96 ± 5.03	13.50 ± 1.38	17.50 ± 6.69	0.00 ± 0.00
DES	10	4/6	36.30 ± 13.95	28.63 ± 22.66	9.00 ± 0.94	20.95 ± 6.28	0.30 ± 0.48
EDE	23	6/17	44.5 ± 15.41	34.34 ± 24.02	4.54 ± 1.93	12.48 ± 6.51	2.04 ± 2.42
ADDE	21	5/16	50.29 ± 12.48	32.34 ± 17.23	3.45 ± 1.41	2.01 ± 1.85	3.29 ± 2.74

[a]HC = healthy control; EDE = evaporative dry eye; ADDE = aqueous-deficient dry eye; DES = dry eye symptom; mean ± SD.

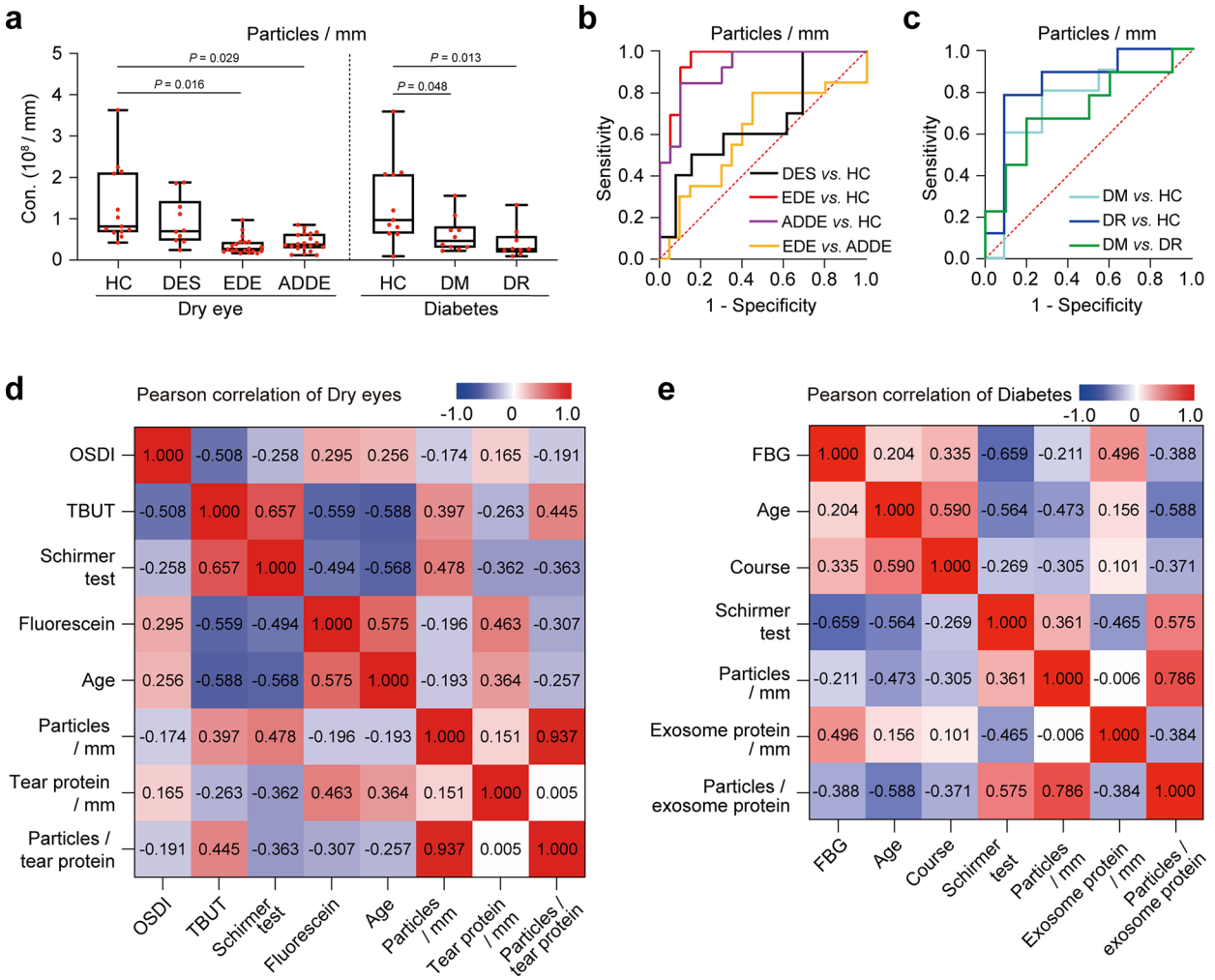

Figure 2. Characterizations of tear exosomes for clinical applications. (a) Scatter diagram showing exosomal particle levels among dry eye subtypes, diabetes patients with or without retinopathy, and healthy donors. Particle levels were defined as the exosome amount per millimeter of a test strip. *P*-value was obtained from Kruskal–Wallis one-way ANOVA. (b) ROC curve of the particle level for dry eye classification analysis. (c) Construction of ROC curve for advanced diabetes monitoring using the exosomal index of the particle concentration. (d, e) Pearson correlation matrix for particle and protein amounts of samples and clinical parameters. Cases for dry eye (panel d) and diabetes (panel e) studies were included, respectively.

MISEV2018[34] guidelines. All tests show significant protein bands of CD9, CD63, CD81, and Alix in iTEARS and PEG exosomes. In contrast, the Calnexin band was not observed for all samples except PEG (Figure 1n), indicating the superiority of iTEARS for tear-exosome purification. Considering the time consumed, iTEARS can obtain exosomes within 5 min, which is much faster than SEC (roughly 30 min), UC (1–3 h), and PEG (overnight). Overall, these results indicate that our platform can effectively isolate tear exosomes for downstream detection.

On-Device Clinical Detection of Tear Exosomes. To better understand the role of exosomes in disease classification,

https://doi.org/10.1021/acsnano.2c02531
ACS Nano XXXX, XXX, XXX–XXX

Table 2. Clinical Data of Diabetes Patients[a]

Group	n	Gender (M/F)	Age (years)	Course (year)	BMI(kg/m^2)	FBG (mM)	HbA1c (%)	Schirmer I test
HC	11	4/7	30.27 ± 3.95	0	20.73 ± 2.60	4.91 ± 0.17	DNT	26.68 ± 4.65
DM	10	6/4	57.91 ± 16.04	5.15 ± 5.69	23.97 ± 3.34	9.04 ± 4.87	10.64 ± 2.25	11.11 ± 6.55
DR	9	7/2	53.56 ± 13.66	15.00 ± 9.72	22.72 ± 3.84	8.67 ± 3.36	9.88 ± 2.69	15.11 ± 10.75

[a]HC = healthy control; DM = diabetes mellitus; DR = diabetic retinopathy; DNT = do not test; mean ± SD.

tear exosomes were systematically analyzed and applied in distinguishing DED subtypes since DED is a multifactorial ocular surface disease that significantly impacts daily life.[35] According to the tear secretion volume and ocular surface signs specified in the international Dry Eye Workshop Report,[36] DED is classified into two subtypes, including ADDE and EDE. Commonly, DED diagnosis requires subjective symptoms and objective signs, including the Ocular Surface Disease Index (OSDI) questionnaire, tear breakup time (TBUT), ocular surface staining, and Schirmer's test. Subjects complaining of dry eye symptoms (DES) but without positive diagnostic results were included as negative controls. Our clinical examinations showed that females and older people are more susceptible to developing DED. The subjective and objective tests could distinguish between control and DED subcohorts (Table 1 and Table S1). Nevertheless, current diagnostic assessments of DED subtypes are weakly correlated with subjective symptoms and signs.[37,38]

It has been reported that cancer patients have a higher exosome concentration in urine and plasma, possibly because tumor cells secrete exosomes to communicate with adjacent and distant cells.[39] Here, we hypothesized that the pathological status of DED might be associated with the changes in exosomes secreted by ocular cells. Because the volume of tear flow varied among patients and was not easy to calculate directly, we used Schirmer paper for microsampling teardrops and quantified the tear volume indirectly with the moistened length (*ca.* 2.5 mm for 1.0 μL sample[7]). HC group had the highest exosome concentration (particles per millimeter of the strip), while ADDE produced more proteins in tears (Figure 2a and Figure S5a). By calculating an area under the curve (AUC) in the receiver operating characteristic (ROC) curves, we showed that the particle level could help to discern dry eye but failed to distinguish the DED subcohorts (Figure 2b and Table S2). We observed an excellent performance in subtype discrimination when considering the tear protein and the particles-to-protein ratio (Figure S5a,b). Moreover, there was no significant difference between the HC and DES groups in the clinical examinations (except for TUBT) or particle/protein measurements.

As another application in studying the role of tear exosomes in tracking disease progress, the iTEARS was used to analyze samples from diabetes patients with or without retinopathy. Diabetes mellitus (DM) is one of the most important medical challenges, characterized by reduced insulin synthesis or sensitivity and abnormal glucose metabolism.[40] Individuals with DM have an increased risk for age-associated comorbidities such as progressive vascular inflammation and blood−retina barrier breakdown in the retina, which are critical initiating factors in the pathogenesis of diabetic retinopathy (DR).[41] Previous work also showed that the tear contents in DR vary with disease duration, as diabetes is one of the critical risk factors for DR,[42] although, with limited exosome-based reports, it is essential to see how the tear exosomes contribute to the development and severity of such an age-associated disease.

The HC, DM, and DR cohorts were selected to assess differences in tear exosomes. The patient and healthy group with a statistical difference in age were included, according to the fact that diabetes is a chronic age-associated degenerative metabolic disease, and the older ones have the trend toward diabetes (Table 2). We found that the averages of body mass index (BMI), fast blood glucose (FBG) level, and glycosylated hemoglobin (HbA1c) level are comparable between DM and DR groups. Besides, there is no significant increasing age trend during DM to DR, but one with diabetes has to spend additional disease courses on developing retinopathy (Table S3). In serum-based studies, a higher level of exosomes in diabetes was reported,[43] which could contribute to the vascular damage in DR by a complement activation manner.[44] As with DED analysis, exosome and protein concentration were defined as particle amounts and protein quantity to the recorded length of the test strip, respectively, to offset the individual difference in tear secretion and collection. In this case, the HC group obtained tear exosomes with higher particle concentration but lower protein levels than those in the two diabetes groups (Figure 2a and Figure S5c). Even without a statistical difference, a slight decrease in particle and protein concentration was observed from DM to DR. Additionally, HC had the highest index when we modified the data from the particle to the protein level (Figure S5d). We further quantitatively evaluated the diagnostic ability of these exosomal metrics using ROC curve analysis. As depicted in Figure S5d and Table S4, the particle-to-exosome protein ratio showed the best diagnostic performance with AUC of 0.945 and 0.960 for distinguishing DM and DR to HC, respectively. Particle and exosome protein levels had AUCs of 0.711 and 0.700 compared to those of the DM and DR groups (Figure 2c and Figure S5c).

Besides, there is limited influence on particle diameter among disease subtypes or during disease progression (Figure S6). We also explored the potential of exosomal parameters in clinical diagnosis (Figure 2d,e). Results showed that the particle-to-protein ratio had a significant positive relationship with particle concentration, but there was no correlation between them and the protein level. Notably, as for dry eye, TBUT and Schirmer test results showed a significant positive correlation with particle amount, while fluorescein staining and age were negatively correlated with particle-to-tear protein ratio. In diabetes cases, FBG, age, and disease course were negatively related to the particle amounts but favorable to the exosome protein levels, contrary to the Schirmer test results. In short, both dry eye and diabetes patients demonstrated reduced tear-exosome concentrations to various degrees; however, the underlying mechanisms need to be further explored.

Proteomic Analysis of Exosomes for Classification of Dry Eye Disease. No single or panel protein markers were reported to diagnose the DED subtypes. Hence, as a proof of

https://doi.org/10.1021/acsnano.2c02531
ACS Nano XXXX, XXX, XXX−XXX

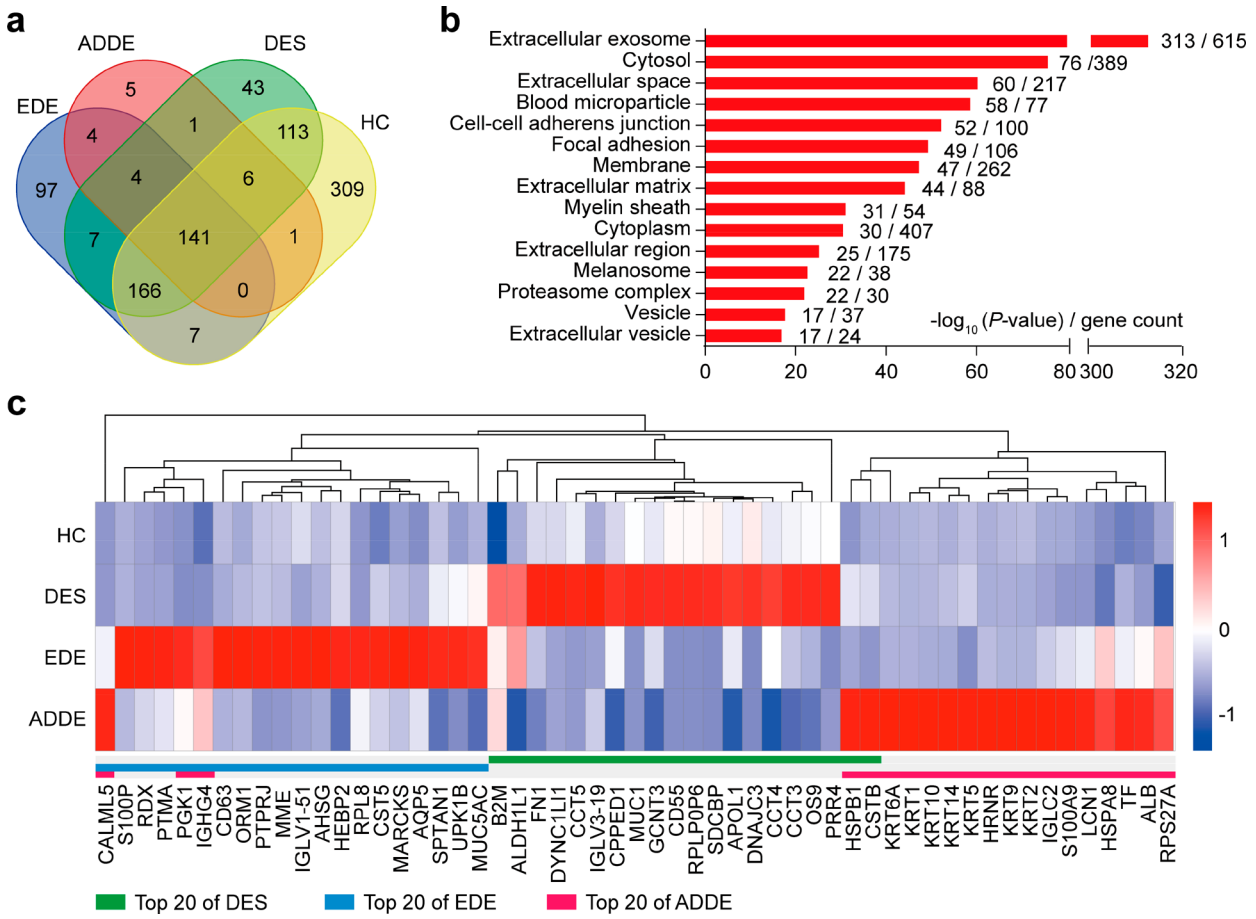

Figure 3. Proteomic profiling of tear exosomes for classification of dry eye. (a) Venn diagram of proteins identified in EDE, ADDE, DES, and HC groups. (b) Cellular components of 904 proteins from all groups. (c) Heat map of the top 20 upregulated proteins (*vs.* healthy control) in each dry eye group. The color key shown is based on the relative intensity transferred to the Z-score.

concept, we performed proteomics analysis to demonstrate the clinical utility of iTEARS-purified tear exosomes in biomarker discovery. By analyzing exosomes from pooled samples, 904 proteins were identified (source data 1), among which 450 were quantifiable (quantifiable proteins indicate that at least one comparison group has quantitative information). The Venn diagram showed 141 proteins expressed in four groups (Figure 3a). More proteins were detected in HC (743) when compared to ADDE (162), EDE (426), and DES (481), which could be concluded by a high expression of some disease-related proteins in the dry eye pathological process.

To evaluate the efficiency of exosome purification, we performed a gene ontology (GO) analysis of all identified proteins and found that most were enriched in extracellular exosomes (Figure 3b). The exosomal markers reported previously were also detectable, which showed different expression patterns when comparing DED subcohorts with the HC group (Table S5). We also detected the vesicle trafficking and biogenesis-related proteins such as the RAB family protein (RAB35, RAB21, RAB25, RAB10, RABEP2, and RAB21) and vacuolar protein sorting-associated protein 4B (VPS4B) in the HC group (Table S6). We further analyzed the signature proteomes of each group by comparing the differentially expressed proteins. The 20 most upregulated proteins in each group are selected and shown in Figure 3c. Compared to HC, the three most upregulated proteins in EDE, specifically, protein S100-P (S100P), calmodulin-like protein 5 (CALML5), and radixin (RDX), are involved in immunological reactions, epidermis development, and cell migration (Table S7). CALML5, Keratin type II cytoskeletal 6A (KRT6A), and cystatin-B (CSTB) were the most upregulated proteins in the ADDE. Besides, T-complex protein 1 subunit epsilon (CCT5), cytosolic 10-formyltetrahydrofolate dehydrogenase (ALDH1L1), and mucin-1 (MUC1) were observed to be upregulated slightly in DES. In addtion, because calcium-binding proteins play vital roles in epidermal differentiation and signal transduction, CALML5 was also found to be upregulated in saliva from pSS patients,[14] indicating its diagnosis potential as a biomarker in DED classification. Besides the high expression of CALML5 in DED subcohorts, inflammatory-associated proteins, including S100P (EDE) and KRT6A (ADDE), also showed significant upregulation in a subtype-specific pattern.

We also found the elevated expressed proteins were involved in the biological processes related to acute inflammatory response, epithelial cell development, and transport across the plasma membrane in EDE (Figure S7a), while defense response against bacterium and antimicrobial humoral response in ADDE was found (Figure S7b). Furthermore, the glycoprotein metabolic process and neutrophil-mediated immunity were elevated in the DES group (Figure S7c). These findings suggest that DES behaves more like healthy controls besides certain protein expressions. Our methodology can identify and implement additional biomarkers as potential non-

https://doi.org/10.1021/acsnano.2c02531
ACS Nano XXXX, XXX, XXX−XXX

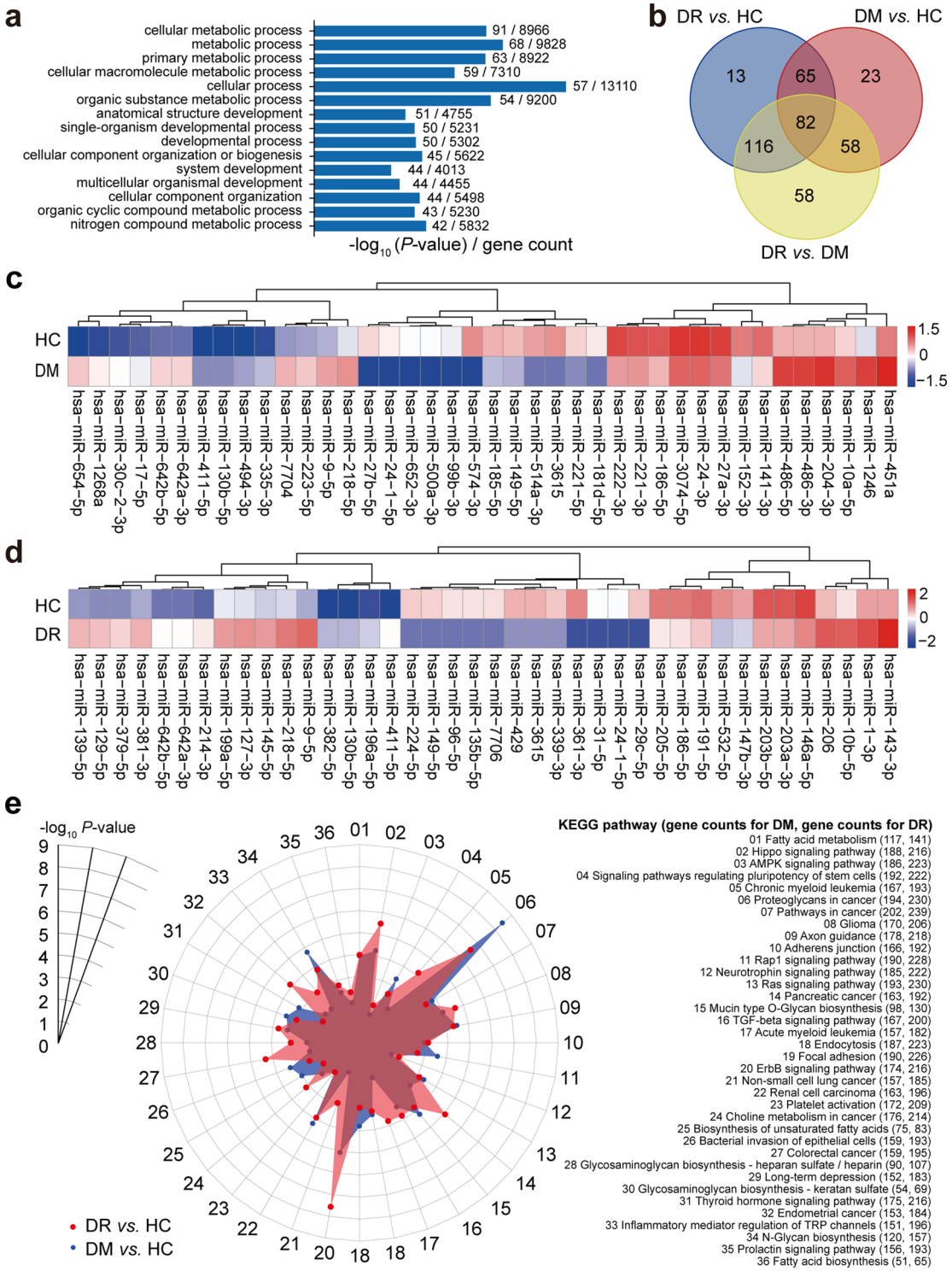

Figure 4. Differentially expressed genes (DEGs)-based analysis comparing the miRNA profiling of tear exosomes in diabetes mellitus and diabetic retinopathy. (a) The enriched biological processes from the identified exosomal miRNAs. (b) Venn diagram of the DEGs profile when compared with every two groups. (c) Heat map of the top 20 upregulated DEGs and top 20 downregulated DEGs for DM compared to HC. The DEGs identified in both groups were selected. The color bar indicates the relative expression level. (d) The comparison of the exosomal miRNA profiles between DR and HC. (e) The differences of enriched KEGG pathways between DM and DR. The statistical enrichment scores were defined as − log (*P*-value).

invasive diagnostic tools. Altogether, these findings may increase diagnostic accuracy when evaluating dry eye symptoms, identifying patients with DED, and monitoring disease progression.

Transcriptomic Analysis of Exosomal miRNA in Diabetes Mellitus and Diabetic Retinopathy. More studies demonstrated that exosomes could transfer miRNAs between organs to alternate the gene expression and functions in recipient cells and serve as a non-invasive biomarker for

https://doi.org/10.1021/acsnano.2c02531
ACS Nano XXXX, XXX, XXX−XXX

disease detection.[45] During the past decade, researchers have supported the role of blood exosomal miRNAs in metabolic complications such as glucose intolerance, inflammation, and endothelial dysfunction.[46,47] Still, many aspects of those from tears remain to be elucidated. Thus, miRNA profiling was performed to see the changes in exosomal cargo and function during the disease progression of diabetes. After using iTEARS and small RNA sequencing, we identified 484 miRNAs in tear exosomes (354 for HC, 344 for DM, and 322 for DR; source data 2). The miRNA distribution among the three groups exhibited a similar pattern, but the disease-dependent biases are higher than that in the healthy group (Figure S8a). Targets of these miRNAs were first predicted from their functions in biological processes, from which the enrichments of a series of metabolic-related processes could be concluded (Figure 4a).

We then compared the total miRNAs across these cohorts, and the results revealed that 228 and 276 differential expressed genes (DEGs) were identified for DM and DR, respectively (Figure 4b). To identify unique miRNAs, DEGs shared in every two groups were selected (Figure S8b,c). The top 20 dysregulated miRNAs in either upregulated or downregulated directions were shown in Figure 4c,d and Table S8. Among these, several potential markers reported in DM and DR studies were also detected in our exosome-based results, which involve inflammatory response,[48] angiogenesis,[49] glucose metabolism,[50] and insulin sensitivity.[51] Mainly, exosomal miRNAs such as miR-218-5p, miR-451a, and miR-486-5p showed a significant increase, while the expression levels of miR-221-3p, miR-222-3p, and miR-24-3p were decreased in DM compared with the control. As for DR, the upregulation of miR-145-5p, miR-214-3p, and miR-9-5p and the downregulation of miR-146a-5p, miR-31-5p, and miR-96-5p, were also observed. More importantly, the specific DEGs identified in DM and DR, including miR-145-5p, miR-214-3p, miR-218-5p, and miR-9-5p, were continuously increasing from healthy control to diabetic cases without and with retinopathy (Figure S9), indicating the diagnostic potential for monitoring disease development.

We finally analyzed the enriched pathway of these disease-dysregulated miRNAs by predicting their targets. Functional annotation of the KEGG pathway revealed common biological pathways in both DM and DR (Figure 4e). As expected, we found that miRNAs significantly affect the diabetic-associated pathways such as energy metabolism (fatty acid metabolism, N-glycan biosynthesis, proteoglycans), insulin secretion (hippo signaling),[52] and insulin resistance (ErbB signaling)[53] in two diabetic cases.[55] Overall, the exosomal miRNAs identified *via* iTEARS reveal strong evidence in the disease-specific biomarker screen and underlying molecular mechanism studies during disease progression.

CONCLUSIONS

Exosomes with membrane structures can encapsulate and protect their cargos, thus becoming a promising source for disease early detection. Tears can be non-invasively and self-collected from patients for exosome analysis. However, the tear-exosome-based disease analysis has rarely been reported so far. Recording exosomes from trace samples for further analysis is necessary in exploring the tear-exosome-based disease world. We have recently developed a harmonic oscillation of a nanopore membrane for the ultrafast exosome isolation system to address the limitation of commercial methods in analyzing samples with narrow volume ranges and time-consuming processes. We have modified and expanded it to perform rapid tear-exosome purification while allowing *in situ* detection and biomarker discovery.

We first report that iTEARS is suitable for purifying small extracellular vesicles, especially exosomes, by characterizing the submicroscopic structures and detecting the specific proteins of tear exosomes. We select 5 mL as the initial volume of 1X PBS to contain teardrops, according to its suitable liquid level in covering the strips in a 15 mL centrifuge tube. The iTEARS processes samples with an extensive range in both volume and dilution, which conclude a limit of process volume of 1 mL for NTA, WB, and on-device detection of the membrane proteins. Compared with the conventional ELISA, iTEARS allows direct immune-targeting of exosomes without precapturing them using additional antibodies or antigens. The differential signals between CD9 and CD81 are probably due to the weaker essential expression and packaging efficiency of CD81 in tear exosomes, which is similar to the WB results. In addition, the different performances of primary antibodies for protein detection might also give different signals. However, both CD9 and CD81 showed linear curves to the input sample volume and a relatively low LOD (0.5−1 mL of sample volume) compared to TSG101, Alix, and Mac-2BP. Additionally, despite the applicability of commercial strategies for tear studies, we demonstrate the isolation and analysis performance of iTEARS in tear sEV yield, purity, and efficiency by a comparative analysis.

In clinical studies, the particles and protein amount per strip wetting length is used to evaluate the exosome level among different cohorts. During disease evaluation, exosomes and proteins are variable in different subtypes, providing anevidence of the tear exosomes in disease diagnosis and monitoring. Abnormal tear secretion might contribute to the elevation of protein concentration in ADDE. The reflex tear secretion induced by excessive aqueous loss and tears instability contribute to the exosome loss in EDE. Additionally, we find the pathological state of dry eye or diabetes both affect tear secretion. A lower concentration of exosomes has been found in all disease groups compared to the healthy control. One possible reason is the limited tear volume-induced hyperosmolality that makes exosomes more susceptible to changing conditions. The diabetes patients are usually excluded from the dry eye cohorts, owing to the Schirmer test scores higher than 5 mm/5 min. Here, we also demonstrate the potential of tear exosomes in revealing the abnormity in the fundus and even in nonocular disease. Generally, in diabetes but not dry eye cohorts, protein concentration after exosome isolation is still at a detectable level and even higher than a control, probably due to the disease-induced changes of protein expression and package within exosomes, suggesting that the changes in protein content may become the non-invasive biomarkers for disease progression monitoring.

Since exosomes are recognized as attractive sources of diagnostic biomarkers, we assume that the tear exosomal cargos could also reflect the variations in physiology and pathology conditions. Using a timsTOF Pro tool, we have profiled the exosomal proteins for dry eye studies. Proteomic data show that vesicle trafficking and biogenesis-related proteins are differentially expressed between healthy and disease groups, which might explain the differential exosome release. Besides the high expression of CALML5 in DED subcohorts, inflammatory-associated proteins are also found

https://doi.org/10.1021/acsnano.2c02531
ACS Nano XXXX, XXX, XXX−XXX

significantly upregulated in a subtype-specific pattern, such as EDE (S100P), ADDE (S100A9), and DES (B2M). Biological process analysis further show that most dysregulated proteins in EDE are enriched in the acute inflammatory response (ORM1, AHSG, and S100A8) and vesicle-mediated transport regulation (TF and RDX), and, as for ADDE, epidermal cell differentiation (HRNR and PGK1) and tissue homeostasis (KRT). Yet, in DES, the enriched biological processes mainly include glycoprotein biosynthetic and metabolic (ALDH1L1). In contrast, limited inflammation and keratinization-related proteins and bioprocesses are found, which reveal the preclinical dry eye status in DES.

We have compared the tear-exosome proteins in healthy donors against tear proteins from previous studies, including de Souza's list[54] and Zhou's proteome.[55] Briefly, compared to those studies, 228 proteins were detected in our work, and 99 proteins were related to the extracellular exosome (Figure S10a). The "GO biological process" pathways (Figure S10b) include translational initiation, SRP-dependent co-translational protein targeting the membrane, and extracellular matrix organization. Inflammation-related pathways (complement activation, NIK/NF-κ B signaling, and antigen processing) were observed by classifying these 228 proteins, providing an attractive resource of biomarkers for understanding the role of exosomes in ocular diseases.

As another essential regulator in disease development, exosomal miRNAs were also considered. Particularly, miR-218-5p, miR-214-3p, and miR-486-5p have shown a strong association with insulin resistance;[56,57] miR-451a is supposed to be involved in fatty acid metabolism pathways.[58] Another three miRNAs (miR-221-3p, miR-222-3p, and miR-24-3p) have been reported to target angiogenesis[59] and vascular dysfunction,[60] whose expression is significantly altered in DM *versus* control. For DR-specific DEGs, dysregulation of miR-24 and miR-31 could be observed in ocular neovascularization.[61] MiR-145 and miR-146 can regulate NFkB signaling and endothelial dysfunction.[62,63] MiR-9 can induce angiogenesis and secretion of insulin, while miR-96-5p hampers the ability of the β-celll to secrete insulin.[64,65] KEGG pathway results further provide the clues associated with diabetes progression. Meanwhile, a high risk of developing pancreatic, renal, and colorectal carcinoma in diabetes patients could be observed. Additionally, the nervous-system-related pathway (glioma and axon guidance pathway) was significantly enriched. The above results indicate that tear exosomes *via* iTEARS could be broadly applied in various disease studies; however, as tear samples from individuals in each study group were pooled before proteome and transcriptome analysis, there may have been a loss of insight into the variability between samples.

In conclusion, we establish the iTEARS for deciphering the secrets of diseases from a teardrop, which reveals the promising role of tear exosomes in disease classification and course monitoring of ocular disorders and other diseases such as neurodegenerative diseases and cancer. By being applied in extended disease types and validated with abundant clinical cases, we anticipate our teardrop-based iTEARS to be the alternative tool for point-of-care-test.

METHODS

Subjects and Tear Sample Collection. The retrospective case-controlled study included patients with dry eye and type 2 diabetes from the Eye Hospital of Wenzhou Medical University (WMU) and is approved by The Ethics Committee of the Eye Hospital of WMU in strict accordance with the contents of the Declaration of Helsinki on Biomedical Research Involving Human Subjects. For dry eye studies, the classification of subtypes is according to the International Dry Eye Workshop Report.[36] For diabetes studies, individuals with DM met the following criteria,[66] and DR was diagnosed by evaluating the retinal fundus photographs of DM patients using a digital retinal camera upon pupil dilation and was classified according to the International Diabetic Retinopathy Severity Scale.[67] The supplementary file describes the grouping criteria of dry eye and diabetes, and the included participants have been listed in Table 1 and Table 2, accordingly. A tear sample was collected by placing a Schirmer paper (Jingming, China) on each eye, and the moistened length was immediately recorded after 5 min of collection or at completion (length reaching at 30 mm in 5 min). The Schirmer strips were transferred to 5 mL of PBS (Gibco, pH 7.4, Thermo Fisher Scientific, Oslo, Norway) and stored at −80 °C until use.

Exosome Isolation and Purification with iTEARS. The tear mixture was eluted from the Schirmer strip by shaking at 4 °C for 30 min and two-step centrifugation (200*g* for 10 min and 3,000*g* for 10 min) to remove cells and other impurities. After filtration with a 0.22 μm syringe filter for further debris removal, the final tear suspension was obtained. Exosomes were subsequently purified with the rapid-isolation system under the negative pressure of 40 kPa and conversion time of 30 s, respectively. After an additional washing with 2 mL of PBS, the final exosomal isolates were reconstituted in ∼150 μL of PBS and stored at −80 °C until analyzing.

Isolation with Other Techniques. Tear suspension was centrifuged for 1 h at 100,000*g* (4 °C) for ultracentrifugation. The obtained pellets were resuspended in PBS for a second 1 h centrifugation at 100,000*g* (4 °C). After removing supernatants, the pellet was finally suspended in 150 μL of PBS. For polymer precipitation, 5 mL of sample mixed well with 1 mL of ExoQuick reagent (EXOCG50A-1, System Biosciences). The mixture was refrigerated overnight at 4 °C. Then the samples were centrifugated at 1,500*g* for 30 min, and the supernatant was discarded. Next, the residual solution was centrifugated at 1,500*g* for 5 min and resuspended in 150 μL of PBS. For size exclusion chromatography, the tear solution was concentrated to 500 μL using 3K Amicon Ultra centrifugal filter devices (Merck Millipore, Darmstadt, Germany). Samples were loaded to the equilibrated size exclusion chromatography column (qEV original, IZON), and 16 sequential fractions of 0.5 mL were eluted by adding PBS. The eluted fractions 8−10 were pooled and concentrated to a final volume of 150 μL.

Nanoparticle Tracking Analysis. NTA was performed on a NanoSight NS300 system (Malvern, USA) with software (Version 3.4, Build3·4·003) according to the previously studies.[29,31] The sample was tracked at a camera level of 16 and a detection threshold of 5.

Transmission Electron Microscopy. Exosome samples were mixed with an equal volume of 4% paraformaldehyde and deposited on Formvar carbon-coated grids (Beijing Zhongkejingyi, China) by floating the grid on 20 μL of mixed sample for 20 min. After removing any excess liquid by filter paper, negative staining was performed with 2% uranyl acetate for 30 s at room temperature. Images were then captured using TEM (Helios Nanolab DualBeam, FEI, USA) at 80 kV.

Western Blot. Protein concentration was measured by Qubit Protein Assay Kit (Invitrogen, USA). For silver staining and WB, samples were loaded on two separate SDS-PAGE Gels (ExpressPlus PAGE Gels, Genscript, USA). After transferring to a poly(vinylidene fluoride) membrane (PVDF; GE, USA), the protein blots were blocked with 5% skim milk for 1 h and incubated with desired primary antibodies (4 °C, overnight). After washing, the PVDF membrane was incubated with either antirabbit or antimouse IgG-HRP secondary antibody (Santa Cruz Biotechnology, USA) (1:3000) at 4 °C for 1 h, before being incubated with HRP chemiluminescent substrate (SuperSignal West Pico chemiluminescent substrate, Thermo Fisher Scientific) and visualized with ECL detection system (Peiqing JS-M8, China). Primary antibodies used for WB and on-device detection are

https://doi.org/10.1021/acsnano.2c02531
ACS Nano XXXX, XXX, XXX−XXX

listed in the Supporting Information. ImageJ (1.8.0, Germany) was used to measure the adjusted intensity of bands after SDS-PAGE.

On-Device Exosome Detection. Tear suspension with indicated volume was processed as described in the isolation section. Incubation with antibody was then performed for 1 h accordingly. After washing with 0.1% PBST, exosomes were incubated with HRP-conjugated secondary antibodies for 30 min, followed by another two washing cycles. Consequently, 3,3′,5,5′-tetramethylbenzidine substrate was added to react with the HRP for 15 min in darkness. The final solution was collected in 96 well plates preloaded with 1 M H_2SO_4 to stop the color reaction. By comparing the optical density value at 450 nm (OD_{450}, BioTek, USA) of different compositions, an incubation time of 30 min and a minimum washing buffer volume of 3 mL were optimized.

Proteomic Analysis. We have pooled the samples and performed the normalization by loading equal protein mass among all groups. We first adjusted the proteins from different tear-exosome samples to the same amount before digestion. Then we have loaded the samples with equal volumes to detect the protein abundance. The 4D label-free quantitative (LFQ) proteomic profiling was performed. The relative quantitative value of each sample was obtained according to the protein LFQ intensity between different samples: when the ratio of LFQ intensity is >1.5, the proteins were regarded as upregulated; when the ratio of LFQ intensity is <1.5, the proteins were considered as downregulated. Information for both proteomics and transcriptomics analysis were detailed in the Supporting Information.

Exosomal miRNA Sequencing. We normalized the cDNA libraries of small RNA with equal mass for sequencing. Briefly, the loading mass of cDNA was balanced by measuring their sequencing libraries concentration *via* Qubit 2.0 and Q-PCR for further sequencing on the Illumina NovaSeq 6000 platform. We have estimated the miRNA expression levels by the transcript per million (TPM) normalization formula: normalized expression = mapped read count/total reads ×1,000,000. Differential expression analysis (DEG) of two samples was performed using the DEGseq (2010) R package. The DEGs were filtrated with the criteria of an adjust P-value < 0.05 and a fold change >2 in either direction unless otherwise stated. We used bioinformatics prediction tools (mirDIP, MicroT-CDS)[68] to test the statistical enrichment of the target gene candidates in KEGG pathways.

Statistical Analysis. We used GraphPad Prism 8 and Origin 2018 software for graphical representation and IBM SPSS Statistics 23 for statistical analyses. The results were presented as the mean ± standard error of the mean (SEM) or standard deviation (SD). Particle, protein, and size differences between every two groups were compared by Kruskal–Wallis one-way ANOVA if not otherwise specified. GO enrichment analysis used Fisher's exact two-sided test to detect differentially expressed proteins. ROC curves were generated from patient profiling data, and the cutoff value was established by calculating the Youden index. P < 0.05 was considered statistically significant.

ASSOCIATED CONTENT

Supporting Information

The Supporting Information is available free of charge at https://pubs.acs.org/doi/10.1021/acsnano.2c02531.

Additional methodology details, supporting figures, and tables (PDF)

AUTHOR INFORMATION

Corresponding Authors

Luke P. Lee − *Department of Medicine, Brigham Women's Hospital, Harvard Medical School, Boston, Massachusetts 02115, United States; Department of Bioengineering, Department of Electrical Engineering and Computer Science, University of California at Berkeley, Berkeley, California 94720, United States; Institute of Quantum Biophysics, Department of Biophysics, Sungkyunkwan University, Suwon, Gyeonggi-do 16419, Korea;* orcid.org/0000-0002-1436-4054; Email: lplee@bwh. harvard.edu

Fei Liu − *Eye Hospital, School of Ophthalmology and Optometry, School of Biomedical Engineering, Wenzhou Medical University, Wenzhou 325027, China; National Clinical Research Center for Ocular Diseases, Wenzhou 325027, China; Wenzhou Institute, University of Chinese Academy of Science, Wenzhou 325001, China;* orcid.org/0000-0001-5259-5753; Email: feiliu@wmu.edu.cn

Authors

Liang Hu − *Eye Hospital, School of Ophthalmology and Optometry, School of Biomedical Engineering, Wenzhou Medical University, Wenzhou 325027, China; National Clinical Research Center for Ocular Diseases, Wenzhou 325027, China;* orcid.org/0000-0001-9884-0312

Ting Zhang − *Eye Hospital, School of Ophthalmology and Optometry, School of Biomedical Engineering, Wenzhou Medical University, Wenzhou 325027, China; Guangdong Provincial Key Laboratory of Biomedical Imaging and Guangdong Provincial Engineering Research Center of Molecular Imaging, The Fifth Affiliated Hospital, Sun Yat-sen University, Zhuhai 519000, China;* orcid.org/0000-0003-4773-2826

Huixiang Ma − *Eye Hospital, School of Ophthalmology and Optometry, School of Biomedical Engineering, Wenzhou Medical University, Wenzhou 325027, China; National Clinical Research Center for Ocular Diseases, Wenzhou 325027, China*

Youjin Pan − *The Second Affiliated Hospital and Yuying Children's Hospital of Wenzhou Medical University, Wenzhou 325027, China*

Siyao Wang − *Eye Hospital, School of Ophthalmology and Optometry, School of Biomedical Engineering, Wenzhou Medical University, Wenzhou 325027, China; National Clinical Research Center for Ocular Diseases, Wenzhou 325027, China*

Xiaoling Liu − *Eye Hospital, School of Ophthalmology and Optometry, School of Biomedical Engineering, Wenzhou Medical University, Wenzhou 325027, China; National Clinical Research Center for Ocular Diseases, Wenzhou 325027, China*

Xiaodan Dai − *Eye Hospital, School of Ophthalmology and Optometry, School of Biomedical Engineering, Wenzhou Medical University, Wenzhou 325027, China; National Clinical Research Center for Ocular Diseases, Wenzhou 325027, China*

Yuyang Zheng − *The Second Affiliated Hospital and Yuying Children's Hospital of Wenzhou Medical University, Wenzhou 325027, China*

Complete contact information is available at: https://pubs.acs.org/10.1021/acsnano.2c02531

Author Contributions

○L.H., T.Z., and H.M contributed equally to this work.

Notes

The authors declare no competing financial interest.

ACKNOWLEDGMENTS

We thank our clinical colleagues involved in the clinical care of the patients reported here. This work was supported by the

National Natural Science Foundation of China (Grant Nos. 21904098, 31741036, and 81800841), the Zhejiang Provincial and Ministry of Health Research Fund for Medical Sciences (Grant No. WKJ-ZJ-1910), the Basic Scientific Research Project of Wenzhou City (Grant No. Y2020202), and the grant from Wenzhou Institute, University of Chinese Academy of Sciences (WIBEZD2017006-05).

REFERENCES

(1) Zhang, P.; Wu, X.; Gardashova, G.; Yang, Y.; Zhang, Y.; Xu, L.; Zeng, Y. Molecular and Functional Extracellular Vesicle Analysis Using Nanopatterned Microchips Monitors Tumor Progression and Metastasis. *Sci. Transl. Med.* **2020**, *12*, No. eaaz2878.

(2) Li, W.; Wang, H.; Zhao, Z.; Gao, H.; Liu, C.; Zhu, L.; Wang, C.; Yang, Y. Emerging Nanotechnologies for Liquid Biopsy: The Detection of Circulating Tumor Cells and Extracellular Vesicles. *Adv. Mater.* **2019**, *31*, No. 1805344.

(3) Shah, R.; Patel, T.; Freedman, J. E. Circulating Extracellular Vesicles in Human Disease. *N. Engl. J. Med.* **2018**, *379*, 958−966.

(4) Gandham, S.; Su, X.; Wood, J.; Nocera, A. L.; Alli, S. C.; Milane, L.; Zimmerman, A.; Amiji, M.; Ivanov, A. R. Technologies and Standardization in Research on Extracellular Vesicles. *Trends Biotechnol.* **2020**, *38*, 1066−1098.

(5) Karns, K.; Herr, A. E. Human Tear Protein Analysis Enabled by an Alkaline Microfluidic Homogeneous Immunoassay. *Anal. Chem.* **2011**, *83*, 8115−8122.

(6) Mishima, S.; Gasset, A.; Klyce, S. D., Jr.; Baum, J. L. Determination of Tear Volume and Tear Flow. *Invest. Ophthalmol.* **1966**, *5*, 264−276.

(7) Yao, Y. N.; Di, D.; Yuan, Z. C.; Wu, L.; Hu, B. Schirmer Paper Noninvasive Microsampling for Direct Mass Spectrometry Analysis of Human Tears. *Anal. Chem.* **2020**, *92*, 6207−6212.

(8) Sonobe, H.; Ogawa, Y.; Yamada, K.; Shimizu, E.; Uchino, Y.; Kamoi, M.; Saijo, Y.; Yamane, M.; Citterio, D.; Suzuki, K.; Tsubota, K. A Novel and Innovative Paper-Based Analytical Device for Assessing Tear Lactoferrin of Dry Eye Patients. *Ocul. Surf.* **2019**, *17*, 160−166.

(9) Giuffrida, M. C.; Cigliana, G.; Spoto, G. Ultrasensitive Detection of Lysozyme in Droplet-Based Microfluidic Devices. *Biosens. Bioelectron.* **2018**, *104*, 8−14.

(10) Park, J.; Kim, J.; Kim, S.-Y.; Cheong, W. H.; Jang, J.; Park, Y.-G.; Na, K.; Kim, Y.-T.; Heo, J. H.; Lee, C. Y.; Lee, J. H.; Bien, F.; Park, J.-U. Soft, Smart Contact Lenses with Integrations of Wireless Circuits, Glucose Sensors, and Displays. *Sci. Adv.* **2018**, *4*, No. eaap9841.

(11) Sempionatto, J. R.; Brazaca, L. C.; García-Carmona, L.; Bolat, G.; Campbell, A. S.; Martin, A.; Tang, G.; Shah, R.; Mishra, R. K.; Kim, J.; Zucolotto, V.; Escarpa, A.; Wang, J. Eyeglasses-Based tear Biosensing System: Non-Invasive Detection of Alcohol, Vitamins and Glucose. *Biosens. Bioelectron.* **2019**, *137*, 161−170.

(12) Tamkovich, S.; Grigor'eva, A.; Eremina, A.; Tupikin, A.; Kabilov, M.; Chernykh, V.; Vlassov, V.; Ryabchikova, E. What Information Can Be Obtained from the Tears of a Patient with Primary Open Angle Glaucoma? *Clin. Chim. Acta* **2019**, *495*, 529−537.

(13) Aqrawi, L. A.; Galtung, H. K.; Guerreiro, E. M.; Ovstebo, R.; Thiede, B.; Utheim, T. P.; Chen, X.; Utheim, O. A.; Palm, O.; Skarstein, K.; Jensen, J. L. Proteomic and Histopathological Characterisation of Sicca Subjects and Primary Sjogren's Syndrome Patients Reveals Promising Tear, Saliva and Extracellular Vesicle Disease Biomarkers. *Arthritis Res. Ther.* **2019**, *21*, 181.

(14) Aqrawi, L. A.; Galtung, H. K.; Vestad, B.; Ovstebo, R.; Thiede, B.; Rusthen, S.; Young, A.; Guerreiro, E. M.; Utheim, T. P.; Chen, X.; Utheim, O. A.; Palm, O.; Jensen, J. L. Identification of Potential Saliva and Tear Biomarkers in Primary Sjogren's Syndrome, Utilising the Extraction of Extracellular Vesicles and Proteomics Analysis. *Arthritis Res. Ther.* **2017**, *19*, 14.

(15) Zhang, T.; Hu, L.; Ma, H.; Ni, F.; Liu, F.; Chen, H. Detection of Tear Components Using Matrix-Assisted Laser Desorption Ionization/Time-of-Flight Mass Spectrometry for Rapid Dry Eye Diagnosis. *J. Proteome Res.* **2020**, *19*, 3644−3651.

(16) Pieragostino, D.; Lanuti, P.; Cicalini, I.; Cufaro, M. C.; Ciccocioppo, F.; Ronci, M.; Simeone, P.; Onofrj, M.; van der Pol, E.; Fontana, A.; Marchisio, M.; Del Boccio, P. Proteomics Characterization of Extracellular Vesicles Sorted by Flow Cytometry Reveals a Disease-Specific Molecular Cross-Talk from Cerebrospinal Fluid and Tears in Multiple Sclerosis. *J. Proteomics* **2019**, *204*, 103403.

(17) Takeuchi, T.; Mori, K.; Sunayama, H.; Takano, E.; Kitayama, Y.; Shimizu, T.; Hirose, Y.; Inubushi, S.; Sasaki, R.; Tanino, H. Antibody-Conjugated Signaling Nanocavities Fabricated by Dynamic Molding for Detecting Cancers Using Small Extracellular Vesicle Markers from Tears. *J. Am. Chem. Soc.* **2020**, *142*, 6617−6624.

(18) Inubushi, S.; Kawaguchi, H.; Mizumoto, S.; Kunihisa, T.; Baba, M.; Kitayama, Y.; Takeuchi, T.; Hoffman, R. M.; Sasaki, R. Oncogenic miRNAs Identified in Tear Exosomes From Metastatic Breast Cancer Patients. *Anticancer Res.* **2020**, *40*, 3091−3096.

(19) An, M.; Wu, J.; Zhu, J.; Lubman, D. M. Comparison of an Optimized Ultracentrifugation Method versus Size-Exclusion Chromatography for Isolation of Exosomes from Human Serum. *J. Proteome Res.* **2018**, *17*, 3599−3605.

(20) Wu, M.; Ouyang, Y.; Wang, Z.; Zhang, R.; Huang, P. H.; Chen, C.; Li, H.; Li, P.; Quinn, D.; Dao, M.; Suresh, S.; Sadovsky, Y.; Huang, T. J. Isolation of Exosomes from Whole Blood by Integrating Acoustics and Microfluidics. *Proc. Natl. Acad. Sci. U. S. A.* **2017**, *114*, 10584−10589.

(21) Gu, Y.; Chen, C.; Mao, Z.; Bachman, H.; Becker, R.; Rufo, J.; Wang, Z.; Zhang, P.; Mai, J.; Yang, S.; Zhang, J.; Zhao, S.; Ouyang, Y.; Wong, D. T. W.; Sadovsky, Y.; Huang, T. J. Acoustofluidic Centrifuge for Nanoparticle Enrichment and Separation. *Sci. Adv.* **2021**, *7*, No. eabc0467.

(22) Grigor'eva, A. E.; Tamkovich, S. N.; Eremina, A. V.; Tupikin, A. E.; Kabilov, M. R.; Chernykh, V. V.; Vlassov, V. V.; Laktionov, P. P.; Ryabchikova, E. I. Exosomes in Tears of Healthy Individuals: Isolation, Identification, and Characterization. *Biochem. (Moscow) Suppl. Ser. B: Biomed. Chem.* **2016**, *10*, 165−172.

(23) Grigor'eva, A. E.; Dyrkheeva, N. S.; Bryzgunova, O. E.; Tamkovich, S. N.; Chelobanov, B. P.; Ryabchikova, E. I. Contamination of Exosome Preparations, Isolated from Biological Fluids. *Biochem. (Moscow) Suppl. Ser. B: Biomed. Chem.* **2017**, *11*, 265−271.

(24) Han, J. S.; Kim, S. E.; Jin, J. Q.; Park, N. R.; Lee, J. Y.; Kim, H. L.; Lee, S. B.; Yang, S. W.; Lim, D. J. Tear-Derived Exosome Proteins Are Increased in Patients with Thyroid Eye Disease. *Int. J. Mol. Sci.* **2021**, *22*, 1115.

(25) Rossi, C.; Cicalini, I.; Cufaro, M. C.; Agnifili, L.; Mastropasqua, L.; Lanuti, P.; Marchisio, M.; De Laurenzi, V.; Del Boccio, P.; Pieragostino, D. Multi-Omics Approach for Studying Tears in Treatment-Naive Glaucoma Patients. *Int. J. Mol. Sci.* **2019**, *20*, 4029.

(26) Guo, S. C.; Tao, S. C.; Dawn, H. Microfluidics-Based on-a-Chip Systems for Isolating and Analysing Extracellular Vesicles. *J. Extracell. Vesicles* **2018**, *7*, 1508271.

(27) Liu, C.; Feng, Q.; Sun, J. Lipid Nanovesicles by Microfluidics: Manipulation, Synthesis, and Drug Delivery. *Adv. Mater.* **2019**, *31*, No. 1804788.

(28) Liu, F.; Vermesh, O.; Mani, V.; Ge, T. J.; Madsen, S. J.; Sabour, A.; Hsu, E. C.; Gowrishankar, G.; Kanada, M.; Jokerst, J. V.; Sierra, R. G.; Chang, E.; Lau, K.; Sridhar, K.; Bermudez, A.; Pitteri, S. J.; Stoyanova, T.; Sinclair, R.; Nair, V. S.; Gambhir, S. S.; et al. The Exosome Total Isolation Chip. *ACS Nano* **2017**, *11*, 10712−10723.

(29) Deng, Z.; Wang, Y.; Hu, L.; Zhu, Q.; Chen, Y.; Chen, J. J.; Chen, J.; Zhang, T.; Seo, T. S.; Liu, F. A Facile, Rapid, High-Throughput Extracellular Vesicles Analytical Platform for Cancer Detection. *Anal. Chim. Acta* **2020**, *1138*, 132−140.

(30) Yang, Q.; Cheng, L.; Hu, L.; Lou, D.; Zhang, T.; Li, J.; Zhu, Q.; Liu, F. An Integrative Microfluidic Device for Isolation and

https://doi.org/10.1021/acsnano.2c02531
ACS Nano XXXX, XXX, XXX−XXX

Ultrasensitive Detection of Lung Cancer-Specific Exosomes from Patient Urine. *Biosens. Bioelectron.* **2020**, *163*, 112290.
(31) Chen, Y.; Zhu, Q.; Cheng, L.; Wang, Y.; Li, M.; Yang, Q.; Hu, L.; Lou, D.; Li, J.; Dong, X.; Lee, L. P.; Liu, F. Exosome Detection *via* the Ultrafast-Isolation System: EXODUS. *Nat. Methods* **2021**, *18*, 212−218.
(32) Chen, Z.; Cheng, S. B.; Cao, P.; Qiu, Q. F.; Chen, Y.; Xie, M.; Xu, Y.; Huang, W. H. Detection of Exosomes by ZnO Nanowires Coated Three-Dimensional Scaffold Chip Device. *Biosens. Bioelectron.* **2018**, *122*, 211−216.
(33) Liu, H.; Yuan, W.; Pang, Q.; Xue, C.; Yan, X. Single-Particle Analysis of Tear Fluid Reveals Abundant Presence of Tissue Factor-Exposing Extracellular Vesicles with Strong Coagulation Activity. *Talanta* **2022**, *239*, 123089.
(34) Théry, C.; Witwer, K. W.; Aikawa, E.; Alcaraz, M. J.; Anderson, J. D.; Andriantsitohaina, R.; Antoniou, A.; Arab, T.; Archer, F.; Atkin-Smith, G. K.; Ayre, D. C.; Bach, J.-M.; Bachurski, D.; Baharvand, H.; Balaj, L.; Baldacchino, S.; Bauer, N. N.; Baxter, A. A.; Bebawy, M.; Beckham, C.; et al. Minimal Information for Studies of Extracellular Vesicles 2018 (MISEV2018): a Position Statement of the International Society for Extracellular Vesicles and Update of the MISEV2014 Guidelines. *J. Extracell. Vesicles* **2018**, *7*, 1535750.
(35) Stapleton, F.; Alves, M.; Bunya, V. Y.; Jalbert, I.; Lekhanont, K.; Malet, F.; Na, K. S.; Schaumberg, D.; Uchino, M.; Vehof, J.; Viso, E.; Vitale, S.; Jones, L. TFOS DEWS II Epidemiology Report. *Ocul. Surf.* **2017**, *15*, 334−365.
(36) Craig, J. P.; Nichols, K. K.; Akpek, E. K.; Caffery, B.; Dua, H. S.; Joo, C. K.; Liu, Z.; Nelson, J. D.; Nichols, J. J.; Tsubota, K.; Stapleton, F. TFOS DEWS II Definition and Classification Report. *Ocul. Surf.* **2017**, *15*, 276−283.
(37) Zhang, J.; Yan, X.; Li, H. Analysis of the Correlations of Mucins, Inflammatory Markers, and Clinical Tests in Dry Eye. *Cornea* **2013**, *32*, 928−932.
(38) Lin, P. Y.; Cheng, C. Y.; Hsu, W. M.; Tsai, S. Y.; Lin, M. W.; Liu, J. H.; Chou, P. Association between Symptoms and Signs of Dry Eye among an Elderly Chinese Population in Taiwan: the Shihpai Eye Study. *Invest. Ophth. Vis. Sci.* **2005**, *46*, 1593−1598.
(39) Verweij, F. J.; Revenu, C.; Arras, G.; Dingli, F.; Loew, D.; Pegtel, D. M.; Follain, G.; Allio, G.; Goetz, J. G.; Zimmermann, P.; Herbomel, P.; Del Bene, F.; Raposo, G.; van Niel, G. Live Tracking of Inter-Organ Communication by Endogenous Exosomes *In Vivo*. *Dev. Cell* **2019**, *48*, 573−589.e4.
(40) Xiao, Y.; Zheng, L.; Zou, X.; Wang, J.; Zhong, J.; Zhong, T. Extracellular Vesicles in Type 2 Diabetes Mellitus: Key Roles in Pathogenesis, Complications, and Therapy. *J. Extracell. Vesicles* **2019**, *8*, 1625677.
(41) Cheung, N.; Mitchell, P.; Wong, T. Y. Diabetic Retinopathy. *Lancet* **2010**, *376*, 124−136.
(42) Ghosh, S.; Ghosh, S.; Azharuddin, M.; Bera, S.; Datta, H.; Dasgupta, A. Change in Tear Protein Profile in Diabetic Retinopathy with Duration of Diabetes. *Diabetes Metab. Syndr.* **2014**, *8*, 233−235.
(43) Freeman, D. W.; Noren Hooten, N.; Eitan, E.; Green, J.; Mode, N. A.; Bodogai, M.; Zhang, Y.; Lehrmann, E.; Zonderman, A. B.; Biragyn, A.; Egan, J.; Becker, K. G.; Mattson, M. P.; Ejiogu, N.; Evans, M. K. Altered Extracellular Vesicle Concentration, Cargo, and Function in Diabetes. *Diabetes* **2018**, *67*, 2377−2388.
(44) Huang, C.; Fisher, K. P.; Hammer, S. S.; Navitskaya, S.; Blanchard, G. J.; Busik, J. V. Plasma Exosomes Contribute to Microvascular Damage in Diabetic Retinopathy by Activating the Classical Complement Pathway. *Diabetes* **2018**, *67*, 1639−1649.
(45) Zhao, J.; Liu, C.; Li, Y.; Ma, Y.; Deng, J.; Li, L.; Sun, J. Thermophoretic Detection of Exosomal microRNAs by Nanoflares. *J. Am. Chem. Soc.* **2020**, *142*, 4996−5001.
(46) Kim, H.; Bae, Y. U.; Lee, H.; Kim, H.; Jeon, J. S.; Noh, H.; Han, D. C.; Byun, D. W.; Kim, S. H.; Park, H. K.; Ryu, S.; Kwon, S. H. Effect of Diabetes on Exosomal miRNA Profile in Patients with Obesity. *BMJ. Open Diabetes Res. Care* **2020**, *8*, e001403.
(47) Pordzik, J.; Jakubik, D.; Jarosz-Popek, J.; Wicik, Z.; Eyileten, C.; De Rosa, S.; Indolfi, C.; Siller-Matula, J. M.; Czajka, P.; Postula, M. Significance of Circulating MicroRNAs in Diabetes Mellitus Type 2 and Platelet Reactivity: Bioinformatic Analysis and Review. *Cardiovasc. Diabetol.* **2019**, *18*, 113.
(48) Suarez, Y.; Wang, C.; Manes, T. D.; Pober, J. S. Cutting Edge: TNF-Induced MicroRNAs Regulate TNF-Induced Expression of E-Selectin and Intercellular Adhesion Molecule-1 on Human Endothelial Cells: Feedback Control of Inflammation. *J. Immunol.* **2010**, *184*, 21−25.
(49) Cordes, K. R.; Sheehy, N. T.; White, M. P.; Berry, E. C.; Morton, S. U.; Muth, A. N.; Lee, T. H.; Miano, J. M.; Ivey, K. N.; Srivastava, D. miR-145 and miR-143 Regulate Smooth Muscle Cell Fate and Plasticity. *Nature* **2009**, *460*, 705−710.
(50) Jordan, S. D.; Krüger, M.; Willmes, D. M.; Redemann, N.; Wunderlich, F. T.; Brönneke, H. S.; Merkwirth, C.; Kashkar, H.; Olkkonen, V. M.; Böttger, T.; Braun, T.; Seibler, J.; Brüning, J. C. Obesity-Induced Overexpression of miRNA-143 Inhibits Insulin-Stimulated AKT Activation and Impairs Glucose Metabolism. *Nat. Cell Biol.* **2011**, *13*, 434−446.
(51) Honardoost, M.; Keramati, F.; Arefian, E.; Mohammadi Yeganeh, S.; Soleimani, M. Network of Three Specific MicroRNAs Influence Type 2 Diabetes through Inducing Insulin Resistance in Muscle Cell Lines. *J. Cell. Biochem.* **2019**, *120*, 1532−1538.
(52) Hwang, J. H.; Kim, A. R.; Kim, K. M.; Il Park, J.; Oh, H. T.; Moon, S. A.; Byun, M. R.; Jeong, H.; Kim, H. K.; Yaffe, M. B.; Hwang, E. S.; Hong, J. H. TAZ Couples Hippo/Wnt Signalling and Insulin Sensitivity through Irs1 Expression. *Nat. Commun.* **2019**, *10*, 421.
(53) Muhammad, I. F.; Borne, Y.; Bao, X.; Melander, O.; Orho-Melander, M.; Nilsson, P. M.; Nilsson, J.; Engstrom, G. Circulating HER2/ErbB2 Levels Are Associated With Increased Incidence of Diabetes: A Population-Based Cohort Study. *Diabetes Care* **2019**, *42*, 1582−1588.
(54) de Souza, G. A.; Godoy, L. M.; Mann, M. Identification of 491 Proteins in the Tear Fluid Proteome Reveals a Large Number of Proteases and Protease Inhibitors. *Genome Biol.* **2006**, *7*, R72.
(55) Zhou, L.; Zhao, S. Z.; Koh, S. K.; Chen, L.; Vaz, C.; Tanavde, V.; Li, X. R.; Beuerman, R. W. In-Depth Analysis of the Human Tear Proteome. *J. Proteomics* **2012**, *75*, 3877−3885.
(56) Bresciani, E.; Saletti, C.; Squillace, N.; Rizzi, L.; Molteni, L.; Meanti, R.; Omeljaniuk, R. J.; Biagini, G.; Gori, A.; Locatelli, V.; Torsello, A. miRNA-218 Targets Lipin-1 and Glucose Transporter Type 4 Genes in 3T3-L1 Cells Treated With Lopinavir/Ritonavir. *Front. Pharmacol.* **2019**, *10*, 461.
(57) Flowers, E.; Aouizerat, B. E.; Abbasi, F.; Lamendola, C.; Grove, K. M.; Fukuoka, Y.; Reaven, G. M. Circulating MicroRNA-320a and MicroRNA-486 Predict Thiazolidinedione Response: Moving Towards Precision Health for Diabetes Prevention. *Metabolism* **2015**, *64*, 1051−1059.
(58) Olioso, D.; Dauriz, M.; Bacchi, E.; Negri, C.; Santi, L.; Bonora, E.; Moghetti, P. Effects of Aerobic and Resistance Training on Circulating Micro-RNA Expression Profile in Subjects With Type 2 Diabetes. *J. Clin. Endocrinol. Metab.* **2019**, *104*, 1119−1130.
(59) Poliseno, L.; Tuccoli, A.; Mariani, L.; Evangelista, M.; Citti, L.; Woods, K.; Mercatanti, A.; Hammond, S.; Rainaldi, G. MicroRNAs Modulate the Angiogenic Properties of HUVECs. *Blood* **2006**, *108*, 3068−3071.
(60) Yang, J.; Chen, L.; Ding, J.; Fan, Z.; Li, S.; Wu, H.; Zhang, J.; Yang, C.; Wang, H.; Zeng, P.; Yang, J. MicroRNA-24 Inhibits High Glucose-Induced Vascular Smooth Muscle Cell Proliferation and Migration by Targeting HMGB1. *Gene* **2016**, *586*, 268−273.
(61) Shen, J.; Yang, X.; Xie, B.; Chen, Y.; Swaim, M.; Hackett, S. F.; Campochiaro, P. A. MicroRNAs Regulate Ocular Neovascularization. *Mol. Ther.* **2008**, *16*, 1208−1216.
(62) Hui, Y.; Yin, Y. MicroRNA-145 Attenuates High Glucose-Induced Oxidative Stress and Inflammation in Retinal Endothelial Cells through Regulating TLR4/NF-KappaB Signaling. *Life Sci.* **2018**, *207*, 212−218.
(63) Cowan, C.; Muraleedharan, C. K.; O'Donnell, J. J., III; Singh, P. K.; Lum, H.; Kumar, A.; Xu, S. MicroRNA-146 Inhibits Thrombin-Induced NF-kB Activation and Subsequent Inflammatory Responses

https://doi.org/10.1021/acsnano.2c02531
ACS Nano XXXX, XXX, XXX−XXX

in Human Retinal Endothelial Cells. *Inves. Ophth. Vis. Sci.* **2014**, *55*, 4944−4951.
(64) Chakraborty, C.; Doss, C. G. P.; Bandyopadhyay, S.; Agoramoorthy, G. Influence of miRNA in Insulin Signaling Pathway and Insulin Resistance: Micro-Molecules with a Major Role in Type-2 Diabetes. *WIREs RNA* **2014**, *5*, 697−712.
(65) Zhuang, G.; Wu, X.; Jiang, Z.; Kasman, I.; Yao, J.; Guan, Y.; Oeh, J.; Modrusan, Z.; Bais, C.; Sampath, D.; Ferrara, N. Tumour-Secreted MiR-9 Promotes Endothelial Cell Migration and Angiogenesis by Activating the JAK-STAT Pathway. *EMBO J.* **2012**, *31*, 3513−3523.
(66) Introduction: Standards of Medical Care in Diabetes—2021. *Diabetes Care* **2020**, *44*, S1−S2.
(67) Wilkinson, C. P.; Ferris, F. L.; Klein, R. E.; Lee, P. P.; Agardh, C. D.; Davis, M.; Dills, D.; Kampik, A.; Pararajasegaram, R.; Verdaguer, J. T. Proposed International Clinical Diabetic Retinopathy and Diabetic Macular Edema Disease Severity Scales. *Ophthalmology* **2003**, *110*, 1677−1682.
(68) Paraskevopoulou, M. D.; Georgakilas, G.; Kostoulas, N.; Vlachos, I. S.; Vergoulis, T.; Reczko, M.; Filippidis, C.; Dalamagas, T.; Hatzigeorgiou, A. G. DIANA-microT Web Server v5.0: Service Integration into MiRNA Functional Analysis Workflows. *Nucleic Acids Res.* **2013**, *41*, W169−W173.

https://doi.org/10.1021/acsnano.2c02531
ACS Nano XXXX, XXX, XXX−XXX